

## Supporting Information

### **Cl<sup>-</sup>-templated coordination polymers constructed from dragonfly-like Ln<sub>4</sub> clusters exhibiting excellent magnetothermal properties**

Xu Bai, Jian Wang, Qin Wang, Ya-Ting Yu, Jia-Nian Li,<sup>a</sup> Hua Me\* and Yan Xu

<sup>a</sup> College of Chemical Engineering, State Key Laboratory of Materials-Oriented Chemical Engineering, Nanjing Tech University, Nanjing 211800, P. R. China

## Experimental Section

### Materials and Methods

All reagents and raw materials used are commercially purchased and have not undergone further purification. Elemental analysis of C, H, and N was performed by a Perkin-Elmer 2400 analyzer. The powder X-ray diffraction pattern of **1-2** was measured at 20°/min with a Bruker D8 diffractometer in the range of  $2\theta = 3-50^\circ$  at room temperature. The infrared spectra of **1-2** were measured by KBr compression method at room temperature in the wavelength range of 4000-400  $\text{cm}^{-1}$ . Thermogravimetric analysis (TGA) is to collect the thermogravimetric curves of two compounds from 25 °C to 1000 °C in a nitrogen atmosphere at the rate of 10 °C  $\text{min}^{-1}$  using a thermogravimetric analyzer Q50. As for the magnetization measurement, we have used the MPS-XL7 SQUID magnetometer to measure the magnetization of **1-2** in the range of 1.8-300 K and 0-7 T.

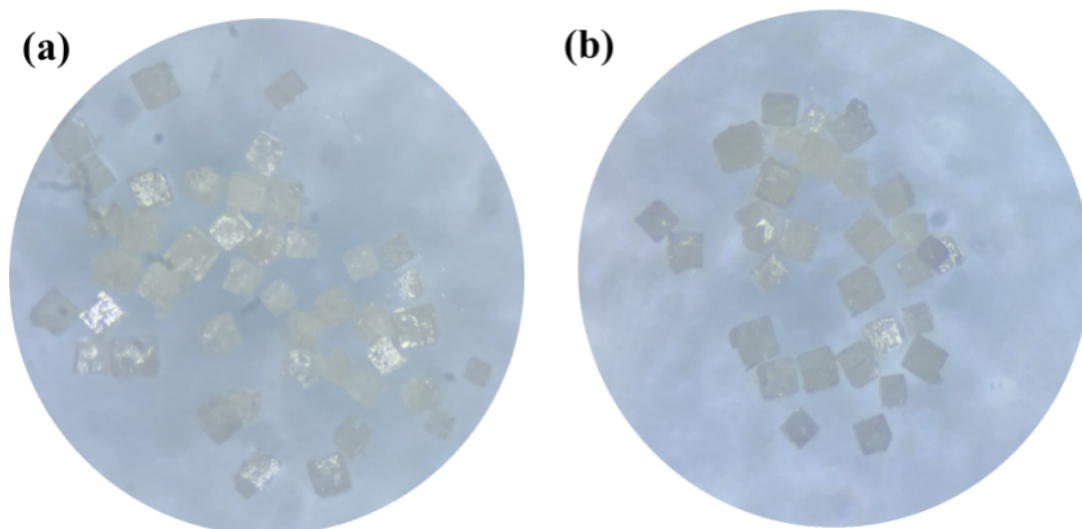


**Fig. S1** The images of (a) **1**; (b) **2** under optical microscope.

## Structure

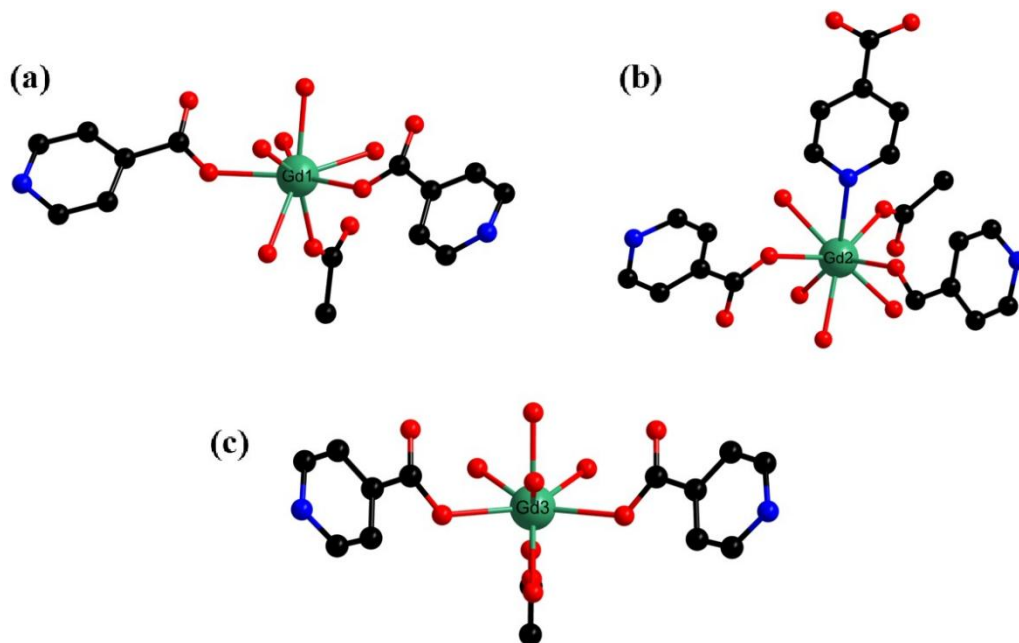


**Fig. S2** The coordination environment of (a) Gd1; (b) Gd2; (c) Gd3 in **1**.

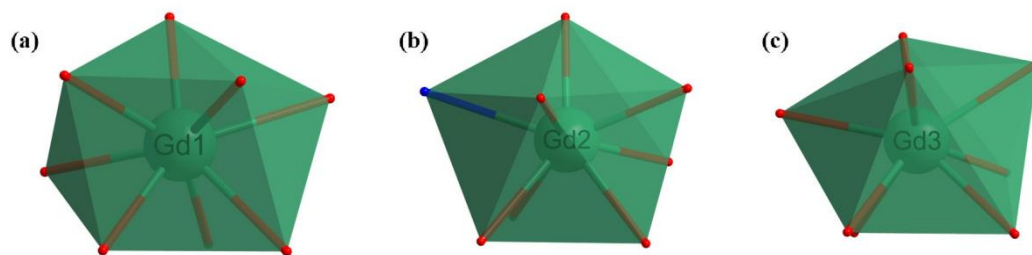


**Fig. S3** The coordination geometry of (a) Gd1; (b) Gd2; (c) Gd3 in **1**.

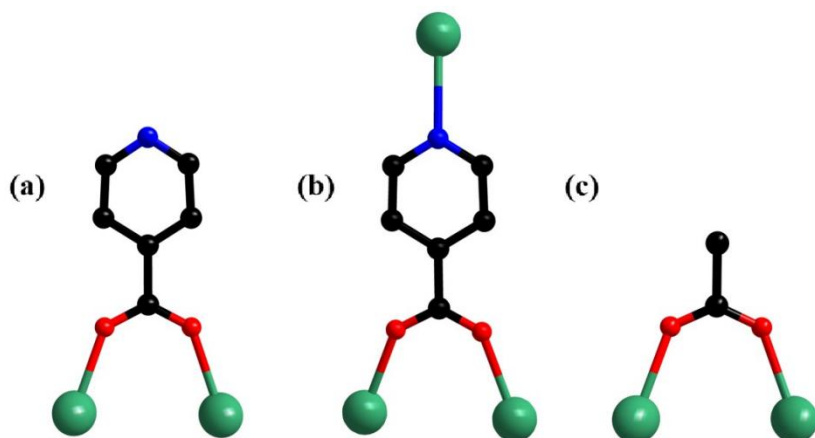


**Fig. S4** (a-b) Two coordination patterns of HIN; (c) Coordination modes of acetate.

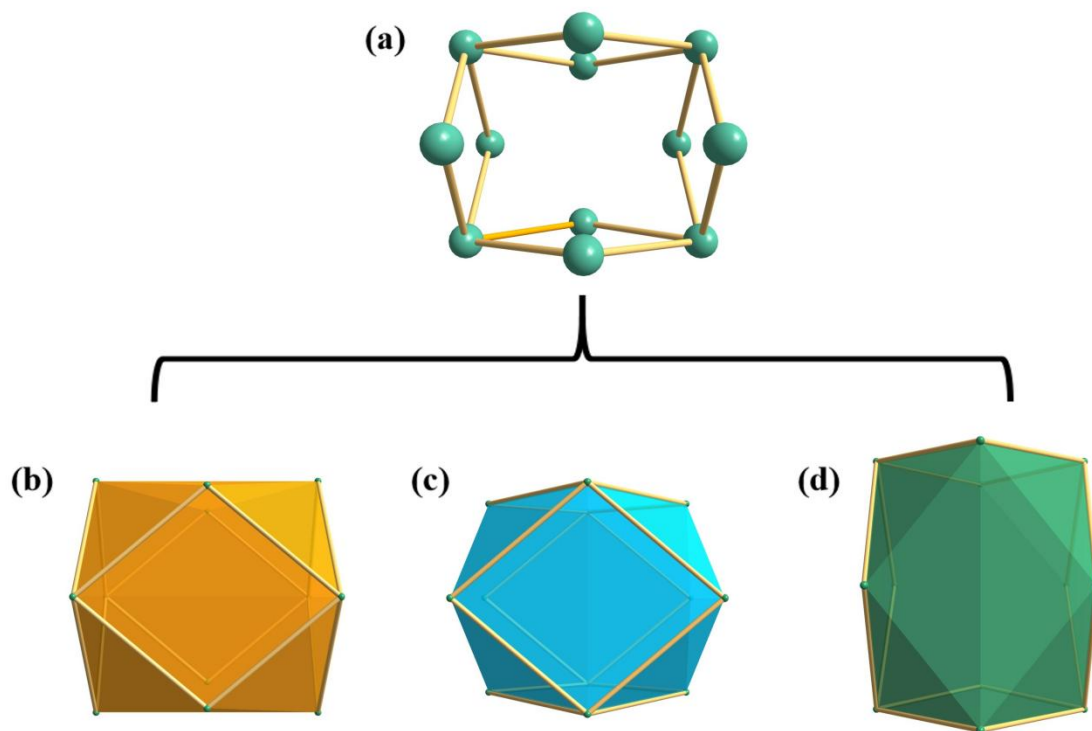


**Fig. S5** (a) Cage structure building unit; (b) Stacking mode 1 (orange); (c) Stacking mode 2 (blue); (d) Stacking mode 3 (green).

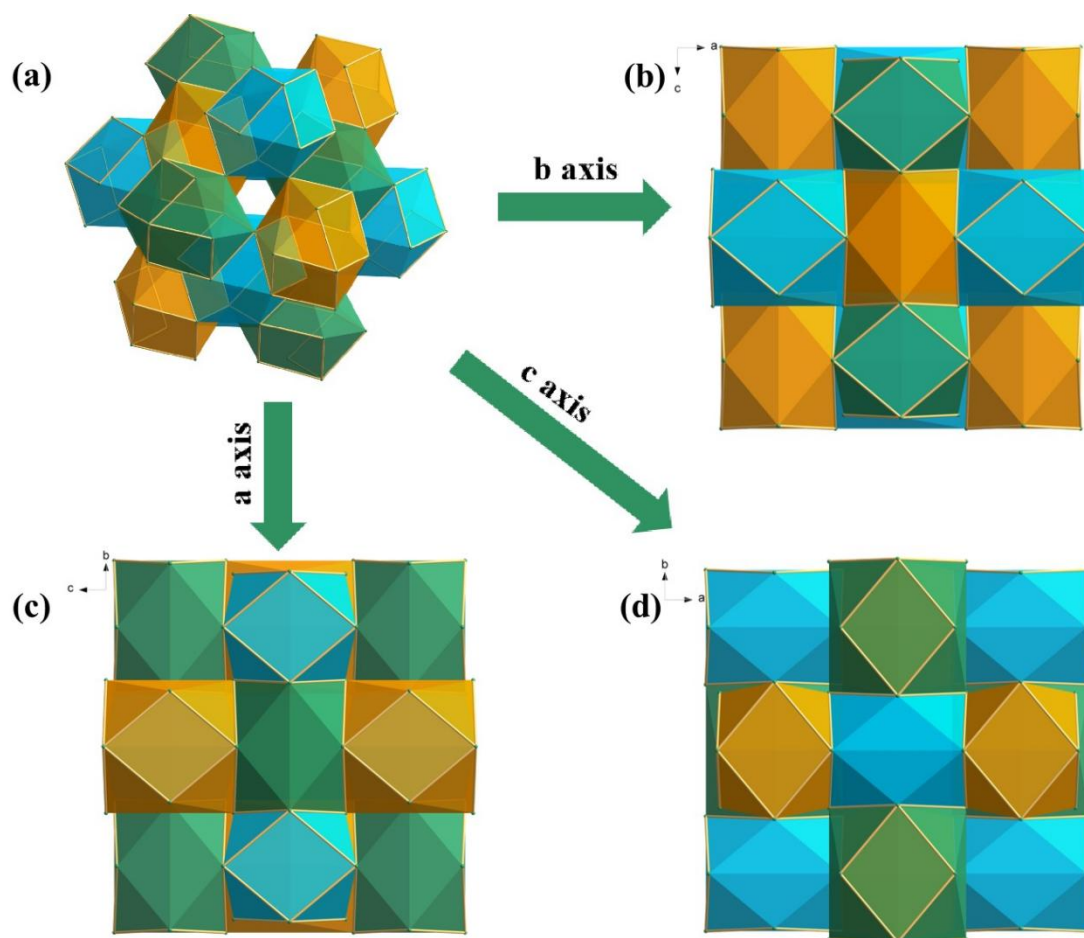


**Fig. S6** (a) 3D structural stacking diagram of **1** observed from (b) a-axis; (c) b-axis; (d) c-axis.

## PXRD patterns

As shown in Fig. S7 and S8,<sup>†</sup> the test results show that the principal diffraction peaks of the two compounds are basically consistent with the corresponding principal diffraction peaks of the single crystal simulation, indicating that the obtained **1-2** are pure phases.

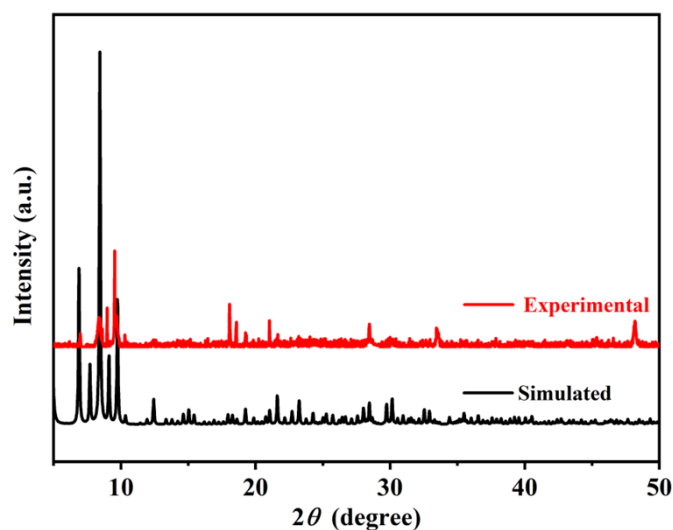


**Fig. S7** The experimental and simulated PXRD patterns of **1**.

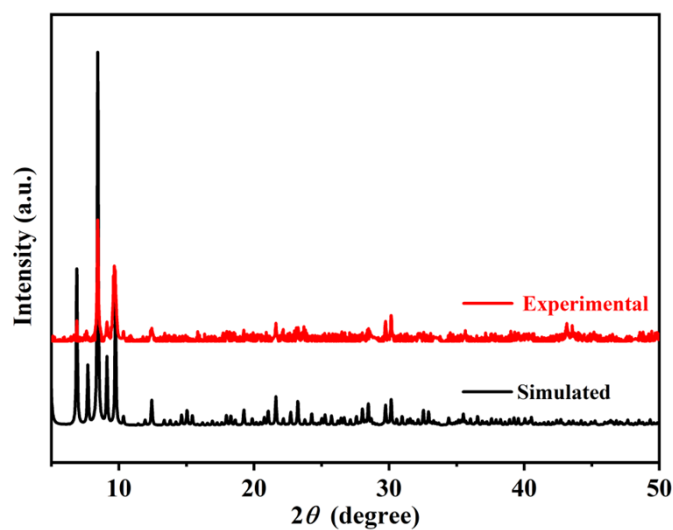


**Fig. S8** The experimental and simulated PXRD patterns of **2**.

## FT-IR patterns

In order to ascertain the infrared spectra of **1-2** under room temperature conditions, the KBr compression method was employed in the wavelength range of 4000-400  $\text{cm}^{-1}$ . Since the infrared spectra of the two compounds in this paper are similar, only compound **1** is introduced here as an example. As shown in Fig. S9,<sup>†</sup> the absorption peak at 3420  $\text{cm}^{-1}$  can be considered to be due to the O-H stretching vibration; the peak at 2924  $\text{cm}^{-1}$  can be attributed to the C-H stretching vibration; the peak at 1617  $\text{cm}^{-1}$  proves the presence of the pyridine ring; and the absorption peaks at 1409  $\text{cm}^{-1}$  and 1548  $\text{cm}^{-1}$  can be attributed to the stretching vibration of the -COO- group; The absorption peak at 773  $\text{cm}^{-1}$  can be considered as the stretching vibration of the Gd-O bond.

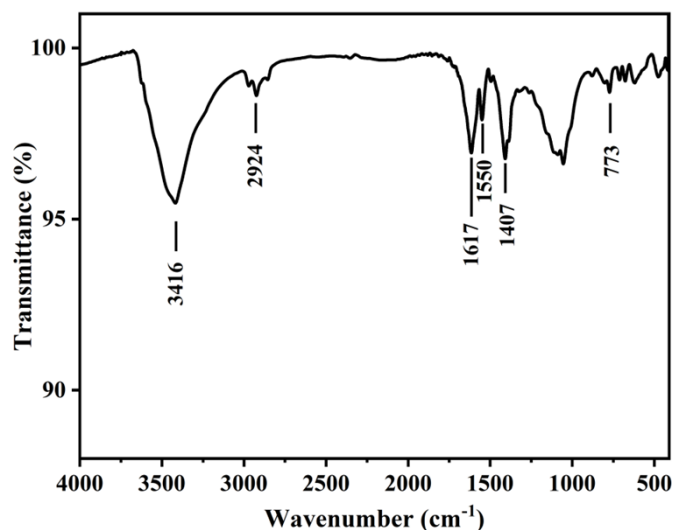


**Fig. S9** The FT-IR spectra of **1**.

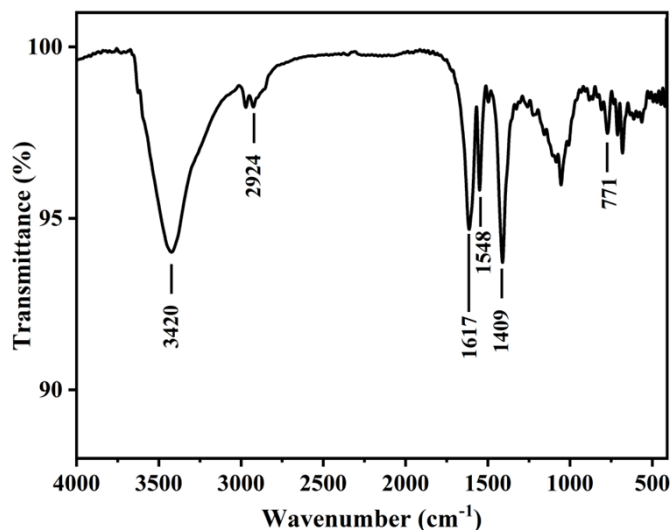


**Fig. S10** The FT-IR spectra of **2**.

## TG

The thermal stability analyses of **1-2** are shown in Fig. S11 and S12,<sup>†</sup> and their curves follow approximately the same trend, which is presented here in detail using only **1** as an example: the whole process can be divided into three phases, the first one being a mass loss of 7.85 % attributed to the loss of seven free water molecules; in the second phase, the decomposition of the organic ligand, HIN, begins. In the third stage, the compound skeleton gradually disintegrates.

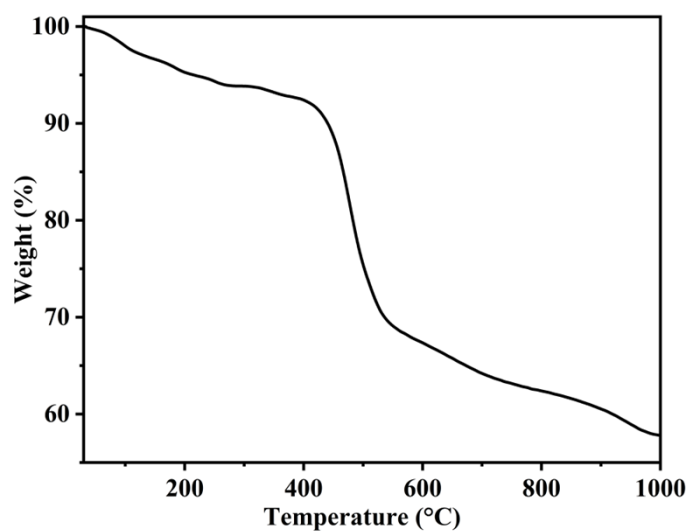


**Fig. S11** The TGA curve of **1**.



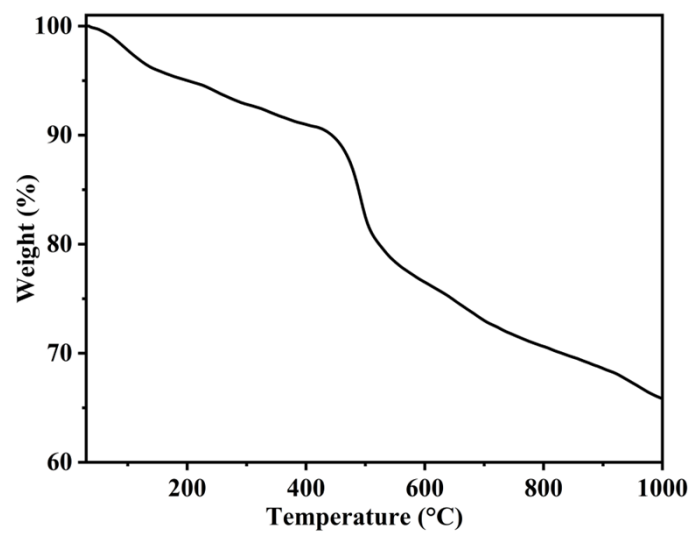


**Fig. S12** The TGA curve of **2**.

## EDS

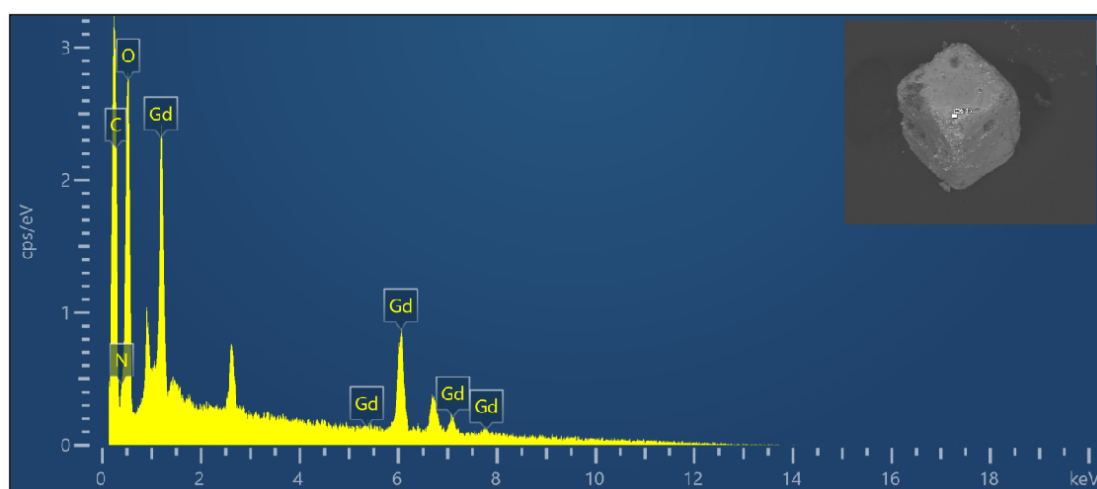


**Fig. S13** The EDS measurement of **1**.

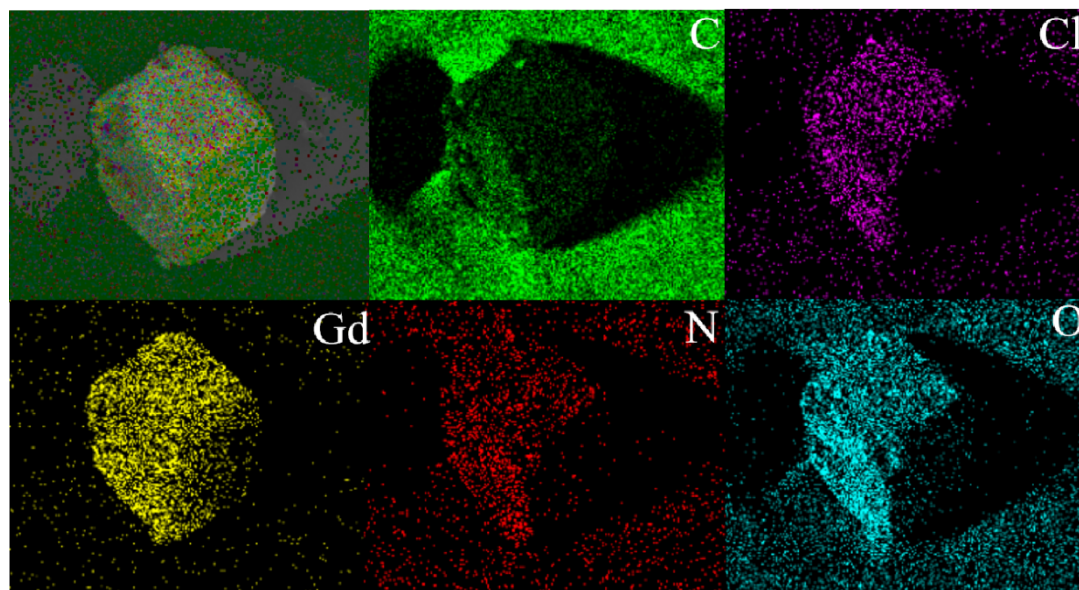


**Fig. S14** The SEM-EDS mapping of **1**.

## Magnetic property

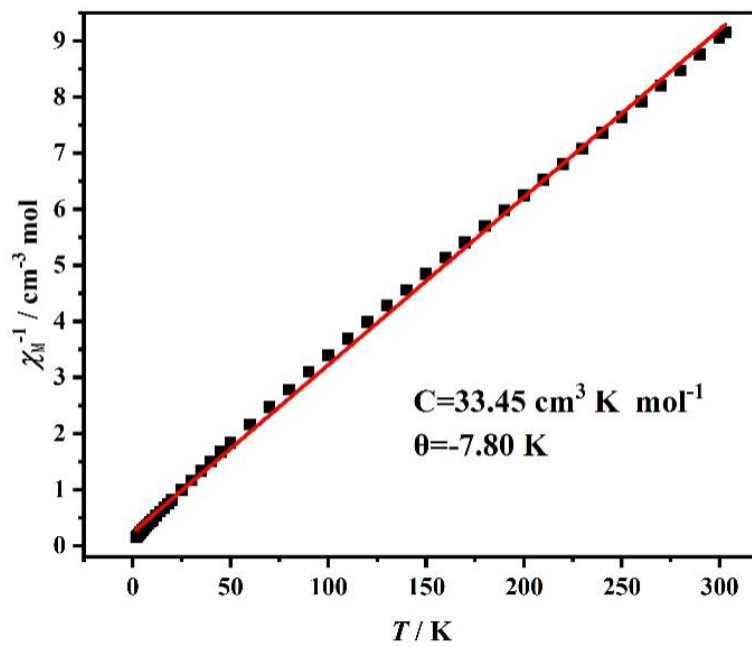


**Fig. S15** The Curie-Weiss fitting curve of **1**.

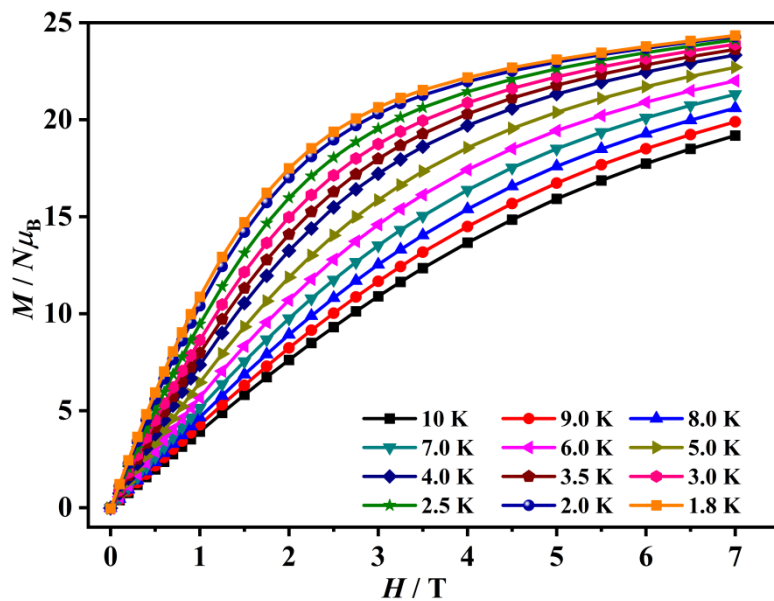


Fig. S16 Field-dependent magnetization in the temperature range of 1.8–10 K for 1.

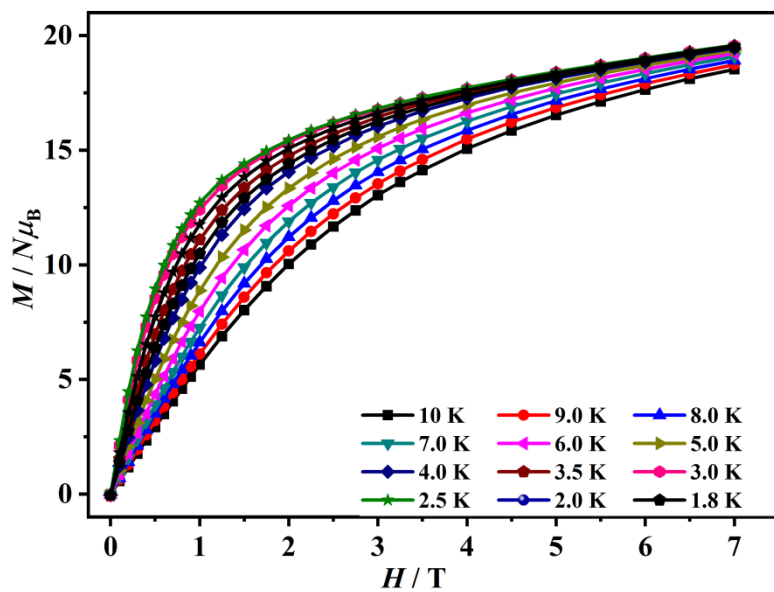


Fig. S17 Field-dependent magnetization in the temperature range of 1.8–10 K for 2.

**Table S1.** Crystallographic data of **1** and **2**.

Compound	<b>1</b>	<b>2</b>
Formula	Gd <sub>4</sub> C <sub>28</sub> H <sub>52</sub> N <sub>4</sub> O <sub>29</sub> Cl <sub>2</sub>	Dy <sub>4</sub> C <sub>28</sub> H <sub>54</sub> N <sub>4</sub> O <sub>30</sub> Cl <sub>2</sub>
Formula Weight	1608.63	1647.65
T (K)	193(2)	193(2)
Crystal system	Cubic	Cubic
Space group	<i>Im</i> -3	<i>Im</i> -3
a (Å)	36.5627(17)	36.2700(14)
V (Å <sup>3</sup> )	48878(7)	47714(6)
Z	24	24
Dc (mg / m <sup>3</sup> )	1.312	1.376
μ (mm <sup>-1</sup> )	3.336	3.841
F (000)	18480	18912
Crystal size (mm <sup>3</sup> )	0.120 × 0.120 × 0.120	0.130 × 0.120 × 0.120
θ range (deg)	0.788 - 24.995	2.101 - 25.025
Limiting indices	-43 ≤ h ≤ 43,	-43 ≤ h ≤ 41,
	-43 ≤ k ≤ 43,	-39 ≤ k ≤ 43,
	-43 ≤ l ≤ 43	-43 ≤ l ≤ 40
Reflections collected / unique	284378	171326
Independent reflections	7556 / R(int) = 0.1412	7366 / R(int) = 0.0748
Completeness	99.9 %	99.8 %
Data / restraints / parameters	7556 / 138 / 303	7366 / 130 / 301
Goodness-of-fit on F <sup>2</sup>	1.026	1.102
R1a, wR2b [I > 2σ(I)]	0.0822 / 0.2182	0.0510 / 0.1467
R1, wR2 (all data)	0.0931 / 0.2237	0.0671 / 0.1598

$$^a R_1 = \sum ||F_o| - |F_c|| / \sum |F_o|. \quad ^b wR_2 = \sum [w(F_o^2 - F_c^2)^2] / \sum [w(F_o^2)^2]^{1/2}.$$

**Table S2.** Bond lengths (Å) and angles (°) of some Gd(III) ions in **1**.

Gd1–O6	2.346(15)	Gd2–O5	2.349(10)
Gd1–O1	2.368(12)	Gd2–O1	2.363(6)
Gd1–O4	2.382(8)	Gd2–O8	2.371(10)
Gd1–O4#1	2.382(8)	Gd2–O10	2.374(12)
Gd1–O3	2.397(9)	Gd2–O4	2.398(8)
Gd1–O3#1	2.397(9)	Gd2–O2	2.413(7)
Gd1–O7W	2.482(16)	Gd2–O5W	2.525(12)
Gd1–O6W	2.55(2)	Gd2–N2#2	2.591(9)
O6–Gd1–O1	146.0(6)	O5–Gd2–O1	93.0(4)
O6–Gd1–O4	80.7(5)	O5–Gd2–O8	141.2(4)
O1–Gd1–O4	71.5(3)	O1–Gd2–O8	91.9(4)
O6–Gd1–O4#1	80.7(5)	O5–Gd2–O10	99.4(5)
O1–Gd1–O4#1	71.5(3)	O1–Gd2–O10	144.9(4)
O4–Gd1–O4#1	69.4(4)	O8–Gd2–O10	98.4(5)
O6–Gd1–O3	97.9(3)	O5–Gd2–O4	75.1(3)
O1–Gd1–O3	92.4(3)	O1–Gd2–O4	70.8(3)
O4–Gd1–O3	72.8(4)	O8–Gd2–O4	142.0(3)
O4#1–Gd1–O3	142.0(4)	O10–Gd2–O4	80.8(4)
O6–Gd1–O3#1	97.9(3)	O5–Gd2–O2	144.3(4)
O1–Gd1–O3#1	92.4(3)	O1–Gd2–O2	70.6(3)
O4–Gd1–O3#1	142.0(4)	O8–Gd2–O2	72.8(4)
O4#1–Gd1–O3#1	72.8(4)	O10–Gd2–O2	80.6(4)
O3–Gd1–O3#1	143.9(6)	O4–Gd2–O2	69.6(3)
O6–Gd1–O7W	141.9(7)	O5–Gd2–O5W	72.9(4)
O1–Gd1–O7W	72.1(6)	O1–Gd2–O5W	71.7(4)
O4–Gd1–O7W	128.6(4)	O8–Gd2–O5W	72.2(4)
O4#1–Gd1–O7W	128.6(4)	O10–Gd2–O5W	143.4(4)
O3–Gd1–O7W	73.8(3)	O4–Gd2–O5W	128.4(3)
O3#1–Gd1–O7W	73.8(3)	O2–Gd2–O5W	126.7(4)
O6–Gd1–O6W	70.1(8)	O5–Gd2–N2#2	78.2(3)
O1–Gd1–O6W	143.9(7)	O1–Gd2–N2#2	144.1(3)
O4–Gd1–O6W	134.7(5)	O8–Gd2–N2#2	75.5(3)
O4#1–Gd1–O6W	134.7(5)	O10–Gd2–N2#2	70.9(4)
O3–Gd1–O6W	77.6(3)	O4–Gd2–N2#2	136.9(3)
O3#1–Gd1–O6W	77.6(3)	O2–Gd2–N2#2	133.2(3)
O7W–Gd1–O6W	71.8(8)	O5W–Gd2–N2#2	72.4(3)

Taking only the bond lengths and angles related to Gd1 and Gd2 as examples

Symmetry transformations used to generate equivalent atoms:

#1  $x, y, z$     #2  $-y+1/2, -z+1/2, -x+1/2$

**Table S3.** Bond lengths (Å) and angles (°) of some Dy(III) ions in **2**.

Dy1–O1	2.344(7)	Dy2–O5	2.313(6)
Dy1–O6	2.353(10)	Dy2–O8	2.334(7)
Dy1–O3	2.359(6)	Dy2–O1	2.342(4)
Dy1–O3#1	2.359(6)	Dy2–O10	2.349(7)
Dy1–O4#1	2.365(5)	Dy2–O4	2.369(5)
Dy1–O4	2.365(5)	Dy2–O2	2.378(5)
Dy1–O5W	2.449(10)	Dy2–O3W	2.432(8)
Dy1–O4W	2.559(13)	Dy2–N2#2	2.587(6)
O1–Dy1–O6	147.6(3)	O5–Dy2–O8	143.6(3)
O1–Dy1–O3	93.60(18)	O5–Dy2–O1	94.0(2)
O6–Dy1–O3	96.28(19)	O8–Dy2–O1	93.1(3)
O1–Dy1–O3#1	93.60(18)	O5–Dy2–O10	97.4(3)
O6–Dy1–O3#1	96.28(19)	O8–Dy2–O10	96.4(3)
O3–Dy1–O3#1	144.0(3)	O1–Dy2–O10	146.1(2)
O1–Dy1–O4#1	71.78(19)	O5–Dy2–O4	73.8(2)
O6–Dy1–O4#1	81.8(2)	O8–Dy2–O4	141.8(2)
O3–Dy1–O4#1	142.4(2)	O1–Dy2–O4	71.7(2)
O3#1–Dy1–O4#1	72.9(2)	O10–Dy2–O4	80.9(2)
O1–Dy1–O4	71.78(19)	O5–Dy2–O2	143.3(3)
O6–Dy1–O4	81.8(2)	O8–Dy2–O2	72.3(3)
O3–Dy1–O4	72.9(2)	O1–Dy2–O2	71.2(2)
O3#1–Dy1–O4	142.4(2)	O10–Dy2–O2	80.9(3)
O4#1–Dy1–O4	69.6(3)	O4–Dy2–O2	69.7(2)
O1–Dy1–O5W	73.3(3)	O5–Dy2–O3W	74.2(3)
O6–Dy1–O5W	139.1(4)	O8–Dy2–O3W	74.2(4)
O3–Dy1–O5W	74.23(17)	O1–Dy2–O3W	72.2(2)
O3#1–Dy1–O5W	74.23(17)	O10–Dy2–O3W	141.7(3)
O4#1–Dy1–O5W	129.6(2)	O4–Dy2–O3W	129.1(3)
O4–Dy1–O5W	129.6(2)	O2–Dy2–O3W	128.0(3)
O1–Dy1–O4W	144.0(4)	O5–Dy2–N2#2	78.1(2)
O6–Dy1–O4W	68.5(5)	O8–Dy2–N2#2	75.1(2)
O3–Dy1–O4W	76.77(18)	O1–Dy2–N2#2	143.5(2)
O3#1–Dy1–O4W	76.77(18)	O10–Dy2–N2#2	70.3(2)
O4#1–Dy1–O4W	134.4(3)	O4–Dy2–N2#2	136.4(2)
O4–Dy1–O4W	134.4(3)	O2–Dy2–N2#2	133.2(2)
O5W–Dy1–O4W	70.7(5)	O3W–Dy2–N2#2	71.4(2)

Taking only the bond lengths and angles related to Dy1 and Dy2 as examples

Symmetry transformations used to generate equivalent atoms:

#1  $x, y, -z$     #2  $-y+1/2, -z+1/2, -x+1/2$

**Table S4.** Continuous Shape Measures (CShM) Calculations of Gd(III) in **1**.

Gd(III) geometry	Gd1 / Gd2 / Gd3
<b>OP-8</b>	31.951 / 31.768 / 31.692
<b>HPY-8</b>	24.658 / 24.313 / 24.016
<b>HBPY-8</b>	17.439 / 17.065 / 16.925
<b>CU-8</b>	10.360 / 9.892 / 9.724
<b>SAPR-8</b>	3.095 / 3.040 / 3.510
<b>TDD-8</b>	<b>0.359 / 0.366 / 0.285</b>
<b>JGBF-8</b>	13.403 / 13.426 / 13.791
<b>JETBPY-8</b>	29.810 / 29.501 / 29.354
<b>JBTP-8</b>	3.065 / 2.874 / 2.818
<b>BTPR-8</b>	2.432 / 2.356 / 2.482
<b>JSD-8</b>	2.284 / 2.112 / 2.184
<b>TT-8</b>	11.050 / 10.441 / 10.382
<b>ETBPY-8</b>	25.852 / 25.253 / 25.409

**OP-8** = Octagon,  $D_{8h}$ ; **HPY-8** = Heptagonal pyramid,  $C_{7v}$ ; **HBPY-8** = Hexagonal bipyramid,  $D_{6h}$ ; **CU-8** = Cube,  $O_h$ ; **SAPR-8** = Square antiprism,  $D_{4d}$ ; **TDD-8** = Triangular dodecahedron,  $D_{2d}$ ; **JGBF-8** = Johnson gyrobifastigium J26,  $D_{2d}$ ; **JETBPY-8** = Johnson elongated triangular bipyramid J14,  $D_{3h}$ ; **JBTPR-8** = Biaugmented trigonal prism J50,  $C_{2v}$ ; **BTPR-8** = Biaugmented trigonal prism,  $C_{2v}$ ; **JSD-8** = Snub dipheneid J84,  $D_{2d}$ ; **TT-8** = Triakis tetrahedron,  $T_d$ ; **ETBPY-8** = Elongated trigonal bipyramid,  $D_{3h}$ .



**Table S5.** Continuous Shape Measures (CShM) Calculations of Dy(III) in **2**.

Dy(III) geometry	Dy1 / Dy2 / Dy3
<b>OP-8</b>	31.761 / 31.826 / 31.309
<b>HPY-8</b>	24.401 / 24.474 / 24.009
<b>HBPY-8</b>	17.409 / 17.195 / 17.027
<b>CU-8</b>	10.418 / 10.841 / 9.859
<b>SAPR-8</b>	3.034 / 3.157 / 3.102
<b>TDD-8</b>	<b>0.407 / 0.438 / 0.329</b>
<b>JGBF-8</b>	13.019 / 13.039 / 13.707
<b>JETBPY-8</b>	29.257 / 29.448 / 28.721
<b>JBTP-8</b>	2.965 / 3.088 / 2.698
<b>BTPR-8</b>	2.411 / 2.500 / 2.439
<b>JSD-8</b>	2.131 / 2.182 / 2.047
<b>TT-8</b>	11.002 / 11.484 / 10.486
<b>ETBPY-8</b>	25.878 / 25.965 / 24.869

**OP-8** = Octagon,  $D_{8h}$ ; **HPY-8** = Heptagonal pyramid,  $C_{7v}$ ; **HBPY-8** = Hexagonal bipyramid,  $D_{6h}$ ; **CU-8** = Cube,  $O_h$ ; **SAPR-8** = Square antiprism,  $D_{4d}$ ; **TDD-8** = Triangular dodecahedron,  $D_{2d}$ ; **JGBF-8** = Johnson gyrobifastigium J26,  $D_{2d}$ ; **JETBPY-8** = Johnson elongated triangular bipyramid J14,  $D_{3h}$ ; **JBTPR-8** = Biaugmented trigonal prism J50,  $C_{2v}$ ; **BTPR-8** = Biaugmented trigonal prism,  $C_{2v}$ ; **JSD-8** = Snub diphendoid J84,  $D_{2d}$ ; **TT-8** = Triakis tetrahedron,  $T_d$ ; **ETBPY-8** = Elongated trigonal bipyramid,  $D_{3h}$ .

**Table S6.** Bond valence calculation (BVS) of compound **1**

Type	Atom1	Atom2	L	$\bar{u}$ (BVS)
$\mu_3$ -OH	O1	Gd1	2.369	1.182
		Gd2	2.363	
		Gd2	2.363	
	O2	Gd2	2.413	1.154
		Gd2	2.413	
		Gd3	2.349	
	O4	Gd1	2.382	1.135
		Gd2	2.397	
		Gd3	2.377	